Prediction of Three-Dimensional Turbulent Mixing in an Ejector

A. D. DeJoode*
Rockwell International, Columbus, Ohio
and
S. V. Patankar†
University of Minnesota, Minneapolis, Minn.

A parabolic three-dimensional finite-difference method incorporating a two-equation model for turbulence closure is used to predict the spreading of a hypermixing turbulent jet within a thrust augmenting ejector. A hypermixing nozzle has an alternating exit causing the formation of streamwise vortices which increases the turbulent mixing. Predicted mainstream velocity profiles for hypermixing jets are compared with experimental data. The formation of the downstream vortices is shown. The selection of initial conditions and the effect of changing initial turbulence levels are also described.

Nomenclature

c	= nozzle element length
c_μ, c_1, c_2	= constants in turbulence model
G	= rate of generation of turbulence kinetic energy
k	= turbulence kinetic energy
p	= cross-stream pressure
$\bar{p}$	= mean pressure
$\Delta\bar{p}$	= pressure change
t	= nozzle exit gap
u_j	= initial jet velocity
x	= mainstream direction
y,z	= cross-stream directions
u	= velocity in x direction
v	= velocity in y direction
w	= velocity in z direction
ϵ	= rate of dissipation of turbulence kinetic energy
η	= normalized y coordinate
μ_t	= turbulent viscosity
ρ	= density
σ_k	= turbulent Prandtl number for k
σ_ϵ	= turbulent Prandtl number for ϵ
τ	= turbulent shear stress

I. Introduction

A. Physical Situation Considered

A THRUST augmenting ejector, Fig. 1, is a device which increases the thrust of a primary jet by the direct transfer of energy from the primary jet to the secondary entrained air drawn from the atmosphere. The mechanism of energy transfer is the turbulent mixing of the two streams at reduced pressure inside a diffuser. If the exhaust flow of a turbojet engine is diverted through a thrust augmenting ejector integrated into an aircraft wing, Fig. 2, the engine thrust is increased, as well as diverted. Thus, the additional thrust required for vertical or short takeoff and landing (V/STOL) capability becomes available. This capability of producing the additional thrust from the cruise engine itself without requiring separate propulsion devices makes the thrust augmenting ejector a very attractive device for use in V/STOL aircraft.

In the early stages of thrust augmenter development, long mixing ducts were used to obtain the complete mixing of the primary and secondary streams needed to acquire significant levels of augmentation. Since long mixing sections are not possible for practical aircraft applications, mechanisms for accelerating the rate of mixing of the primary jet inside the ejector needed to be developed. One such mechanism, the hypermixing nozzle, has been found to be particularly promising[1-3] due to its simple construction and increased rate of mixing. The important features of the hypermixing nozzle and the resulting flowfield are shown in Fig. 3. As shown in the inset, the nozzle exit is divided into several segments. The flow issuing from these segments is given an upward or downward velocity component in an alternating fashion. These velocity components interact with each other to form streamwise vortices, as shown by the arrows on a cross-stream plane in Fig. 3. The figure also shows profiles for the velocity in the main flow direction. The velocity maximum in front of an upward-directed jet segment is seen to be located above the centerline, while the peak velocity in front of the adjacent segment is found below the centerline. In front of the junction

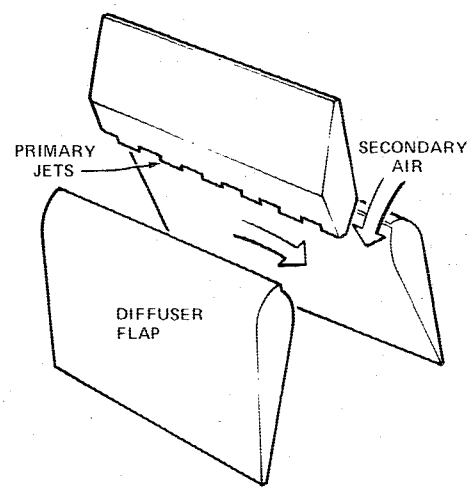

Fig. 1 Typical ejector configuration.

Presented as Paper 77-706 at the AIAA 10th Fluid and Plasma Dynamics Conference, Albuquerque, N. Mex., June 27-29, 1977; submitted Aug. 8, 1977.

Index categories: Jets, Wakes, and Viscid-Inviscid Flow Interactions; Computational Methods.

*Member of Technical Staff, Columbus Aircraft Division. Member AIAA.

†Associate Professor, Department of Mechanical Engineering.

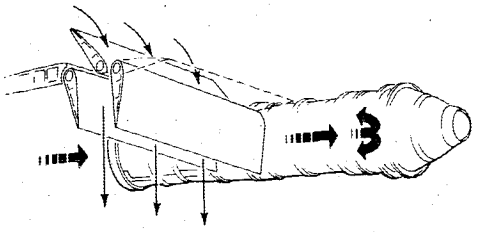

Fig. 2 Turbojet powered wing ejector.

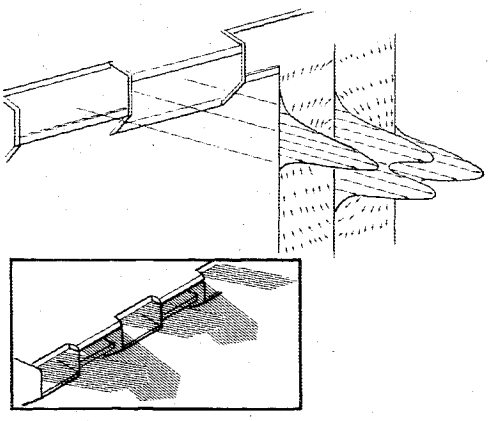

Fig. 3 Hypermixing jet velocities.

of the two segments, the velocity profile has two peaks. This complex velocity field leads to an increased rate of mixing with the surrounding air.

B. Previous Work

The earliest theoretical treatment of a thrust augmenting ejector was a one-dimensional analysis proposed by von Kármán.[4] Later one-dimensional analytic methods[1,3,5] were broadly based on von Kármán's analysis dealing only with mean values of the flow parameters. The ejector is represented by its inlet and diffuser area ratios and the amount of jet mixing is specified by the use of a shape parameter for the mean velocity profile at the ejector exit. Viscous effects are included as empirical pressure loss coefficients. Such parametric methods can increase basic understanding of ejector performance, but are restrictive when used for design purposes due to a need for a large amount of supportive experimental work.

The two-dimensional integral method for ejector analysis developed by Bevilaqua and McCullough[6] does remove the need for a large amount of supportive testing. Their approach is to assume that the velocity distribution is given by the superposition of a self-preserving jet velocity profile on a uniform secondary velocity. This assumption allows the flow equations to be integrated and the resulting equations to be solved together using an empirical relationship to calculate the spreading rate parameter for the jet based upon freejet entrainment data. The method is simple and inexpensive to use and is attractive for preliminary design purposes.

A two-dimensional parabolic finite-difference method developed by Gilbert and Hill[7] using a mixing length model for turbulence eliminates the need for specifying a self-preserving velocity profile shape. This method, modified by the augmenter development group at Rockwell to also include wall jets and an iterative scheme to determine proper initial conditions, works well for the prediction of the performance of simple two-dimensional ejectors.

However, the newer concepts for increasing the rate of entrainment of the primary jets, e.g., hypermixing, are definitely three-dimensional and their turbulent mixing characteristics cannot be predicted adequately with any of the two-dimensional methods previously described. A method capable of modeling the turbulent mixing characteristics of three-dimensional primary jets in terms of the three-dimensional velocity and pressure fields is therefore desirable in order to predict and better understand these complicated mixing flows.

C. Outline of Present Contribution

The aim of the present work is to obtain a numerical solution of the three-dimensional velocity and pressure field in an ejector with hypermixing jets. A complete solution of the three-dimensional elliptic problem will require very large computer storage and computer time. The ejector configuration, however, lends itself to solution by the three-dimensional parabolic-flow procedure of Patankar and Spalding.[8] The method assumes that there is a predominant flow direction so that the flowfield can be computed by marching in the flow direction from an upstream station (where the flow conditions are known) to successive downstream stations. This is akin to solving a two-dimensional problem at every station with consequent saving of computer storage and time.

For the complex flowfield shown in Fig. 3, a sophisticated model is required for turbulence closure. The two-equation turbulence model described by Launder and Spalding[9] is used in the present work. The model incorporates differential equations for the turbulence kinetic energy and its dissipation rate; the local turbulent viscosity is calculated from these quantities. The model has already been used in numerous complex situations and has been shown to produce satisfactory results.

The purpose of the present contribution is to report a numerical solution for the flowfield in a hypermixing jet ejector and to compare it with experiment. The streamwise vortices produced by the hypermixing jets, which have been hypothesized in most of the previous work, are here calculated as a part of the detailed flowfield. The predicted velocity profiles are compared with experimental data.

The details of the mathematical model and the solution method are given in Sec. II. Section III represents the results and their comparison with experimental data.

II. The Prediction Method

A. Governing Equations

The three-dimensional flowfield in the ejector is governed by the continuity equation and the three momentum equations. These equations are regarded as parabolic in the longitudinal coordinate x. This implies that the stresses on the planes normal to the x direction are neglected, and that the x direction velocity is "driven" by the mean pressure $\bar{p}$ over the cross section. These assumptions are the same as the ones used in two-dimensional boundary-layer theory and are explained more fully in Ref. 8. The density is considered to be uniform. The governing equations in Cartesian coordinates are

Continuity

$$\frac{\partial u}{\partial x}+\frac{\partial v}{\partial y}+\frac{\partial w}{\partial z}=0 \tag{1}$$

Momentum

$$\rho u\frac{\partial u}{\partial x}+\rho v\frac{\partial u}{\partial y}+\rho w\frac{\partial u}{\partial z}=\frac{\partial \tau_{yx}}{\partial y}+\frac{\partial \tau_{zx}}{\partial z}-\frac{\mathrm{d}\bar{p}}{\mathrm{d}x} \tag{2}$$

$$\rho u\frac{\partial v}{\partial x}+\rho v\frac{\partial v}{\partial y}+\rho w\frac{\partial v}{\partial z}=\frac{\partial \tau_{yy}}{\partial y}+\frac{\partial \tau_{zy}}{\partial z}-\frac{\partial p}{\partial y} \tag{3}$$

$$\rho u\frac{\partial w}{\partial x}+\rho v\frac{\partial w}{\partial y}+\rho w\frac{\partial w}{\partial z}=\frac{\partial \tau_{yz}}{\partial y}+\frac{\partial \tau_{zz}}{\partial z}-\frac{\partial p}{\partial z} \tag{4}$$

Here, u, v, w are the time-averaged velocity components and the τ's are the turbulent stresses; the corresponding laminar stresses are assumed to be negligible in comparison. To evaluate the turbulent stresses, a turbulence model is used.

B. Turbulence Model

The turbulent stresses are first expressed in terms of a turbulent viscosity μ_t and the velocity gradients. The expression in Cartesian tensor notation is:

$$\tau_{ij} = \mu_t \left(\frac{\partial u_i}{\partial x_j} + \frac{\partial u_j}{\partial x_i} \right) - \frac{2}{3} \rho k \delta_{ij} \tag{5}$$

where δ_{ij} is the Kronecker delta, and k is the kinetic energy of turbulence. For the parabolic flow considered here, the velocity gradients in the x direction (i.e., $\partial u_i / \partial x_1$) will be neglected.

The two-equation turbulence model described by Launder and Spalding[9] expresses the turbulent viscosity μ_t in terms of two parameters, for which two differential equations are solved. The expression for μ_t is

$$\mu_t = c_\mu \rho k^2 / \epsilon \tag{6}$$

where c_μ is a constant, k is the kinetic energy of turbulence, and ϵ is the rate of its dissipation. For the three-dimensional parabolic situation, the governing equations for k and ϵ are

$$\rho u \frac{\partial k}{\partial x} + \rho v \frac{\partial k}{\partial y} + \rho w \frac{\partial k}{\partial z} = \frac{\partial}{\partial y} \left(\frac{\mu_t}{\sigma_k} \frac{\partial k}{\partial y} \right) + \frac{\partial}{\partial z} \left(\frac{\mu_t}{\sigma_k} \frac{\partial k}{\partial z} \right) + G - \rho \epsilon \tag{7}$$

$$\rho u \frac{\partial \epsilon}{\partial x} + \rho v \frac{\partial \epsilon}{\partial y} + \rho w \frac{\partial \epsilon}{\partial z} = \frac{\partial}{\partial y} \left(\frac{\mu_t}{\sigma_\epsilon} \frac{\partial \epsilon}{\partial y} \right) + \frac{\partial}{\partial z} \left(\frac{\mu_t}{\sigma_\epsilon} \frac{\partial \epsilon}{\partial z} \right) + (c_1 G - c_2 \rho \epsilon) \left(\frac{\epsilon}{k} \right) \tag{8}$$

The quantity G is the rate of generation of k by the action of velocity gradients. Since, in the present situation, the only significant gradients are $\partial u/\partial y$ and $\partial u/\partial z$, the expression for G becomes

$$G = \mu_t \left[\left(\frac{\partial u}{\partial y} \right)^2 + \left(\frac{\partial u}{\partial z} \right)^2 \right] \tag{9}$$

The turbulence model involves five empirical constants. According to the recommendation of Launder and Spalding,[9] the following values of the constants are used:

c_μ	c_1	c_2	σ_k	σ_ϵ
0.09	1.44	1.92	1.0	1.3

As seen from Ref. 9, these constants have successfully been used for a wide variety of situations to obtain satisfactory agreement with experiment.

C. Solution Procedure

In the present work, the three-dimensional parabolic-flow method of Patankar and Spalding[8] is used to solve the governing equations. Only a brief description of the method is given here. The method employs a finite-difference marching procedure; from known conditions for an upstream cross section at x, the flowfield at the downstream cross section at $x+\Delta x$ is computed, and this marching process is continued until the domain of interest is covered. Thus, only a two-dimensional computer storage is needed for the cross section under consideration. The finite-difference equations are formed by integrating the differential equations over a small control volume surrounding each grid point. The combined effect of the convection and diffusion (or turbulent stress) is expressed by the hybrid scheme (a combination of the central- and upwind-difference schemes) discussed in Ref. 10. The finite-difference equations are solved by a line-by-line method in which the values of a variable for all the points along a grid line are simultaneously computed by the use of the tri-diagonal-matrix algorithm.

The evaluation of $\bar{p}$ and p requires special mention. For the confined flow in the ejector, the total mass flow rate for any cross section remains the same. The value of $d\bar{p}/dx$ should be such that the resulting values of u give the required mass flow rate. This is arrived at by guessing the value of $d\bar{p}/dx$, solving the momentum equation for u, and then correcting the u's and $d\bar{p}/dx$ to satisfy the overall mass flow requirement. A similar procedure involving the *local* continuity equation is used to find the pressure field p which influences v and w. From a guessed field of p, the cross-stream momentum equations are solved to obtain preliminary values of v and w; these, in general, do not satisfy the continuity equation; therefore, appropriate corrections to the pressure field are computed such that the resulting corrections to the velocity field will make the latter satisfy the continuity equation.

The governing equations are nonlinear and coupled. Thus, the values of the coefficients in the finite-difference equations depend on the values of the variables themselves. Therefore, several iterations are performed during each Δx step until the resulting values of the variables cease to change.

For the ejector configurations studied here, the z direction width of the cross section remains the same, but the y direction dimension increases with x, since the duct is a two-dimensional diffuser. For this reason, it is convenient to use a finite-difference grid in x-η-z coordinates where η is a normalized y coordinate. In the present work, $\eta = (y - y_B)/(y_T - y_B)$ was used, where y_B and y_T are the values of y at the bottom and top walls of the diffuser, respectively. A consequence of the use of this coordinate is that the grid plane of $\eta = 0$ coincides with the bottom wall, while $\eta = 1$ lies along the top wall.

D. Boundary Conditions

The computational boundaries are outlined with dashed lines in Fig. 4. The ejector is considered to be two-dimensional, i.e., there is no change in the y dimension with respect to z and the equal length hypermixing alternating exits

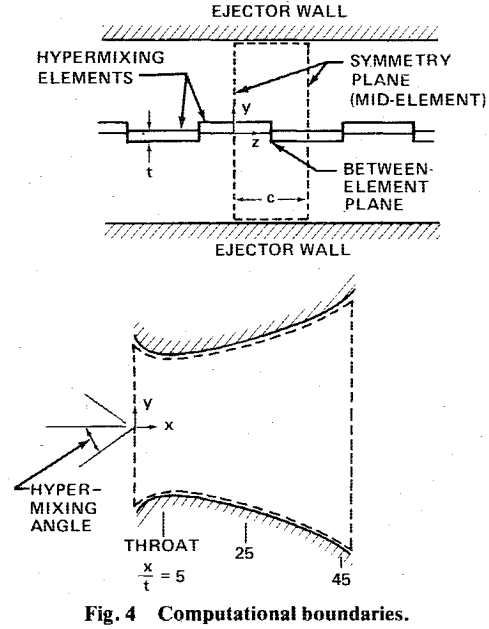

Fig. 4 Computational boundaries.

continue to infinity, thus eliminating the consideration of the ejector endwalls. Upon examining this situation one can see that the center of the streamwise vortex formed would lie along the between-element plane, and each successive cross-stream plane (y-z plane) from midelement to midelement would contain a vortex of equal strength but opposite in direction of rotation. Because of this flow sequence, symmetry planes are used as boundaries at the midelement plane of the hypermixing nozzles. At the symmetry planes the velocity normal to the boundary is zero and the gradients of other quantities normal to the boundary are zero.

The experimental situation, which is used to provide comparison with the computed results, includes, in addition to the hypermixing jets, wall jets on the diffuser walls. However, since the hypermixing jets form the main focus of the present work, the computations have been performed by omitting the wall jets; indeed the friction at the diffuser walls has also been set equal to zero. A parabolic marching computation requires initial conditions as well as boundary conditions. The specification of the initial conditions for the present problem is described in Sec. III B.

III. Results and Comparison with Experimental Data

A. Experimental Apparatus

The basic ejector combines a centerbody nozzle with Coanda jets on the walls in order to provide high augmentation during conversion to wing-borne flight, and to simplify integration with the flap system of the wing. The centerbody jet velocity profiles computed from measured total and static pressure profiles were used to compare with the results from the three-dimensional finite-difference method.

A sketch of the test ejector is shown in Fig. 5. It had a constant span of 20 in., but the components were designed so that the throat width, as well as the flap length and position, could be easily varied. The centerbody nozzle had a hypermixing exit with a nominal length to gap ratio, c/t, of 6.25 and a hypermixing angle of 15 deg. Plane slots were used for the Coanda jets. A slot in each endwall at the ejector throat provided a curtain jet to prevent separation from these surfaces. In the configuration described here, 67% of the primary flow went to the centerbody jet, 14% went to each of the Coanda jets, and the remaining 5% of the flow was divided between the two endwall jets.

The test ejector was supported on four flexible rods attached to a frame. The net thrust was measured with two load cells installed on connecting arms between the frame and lower endwall. High-pressure air was supplied to the primary jets from a single source; but the rate of flow to each nozzle was measured separately, with a calibrated venturi in each of the feed lines. Internal screens and baffles were used to smooth out spanwise variations in the jet velocity and the stagnation pressure was determined with a total pressure probe in the exit of each nozzle.

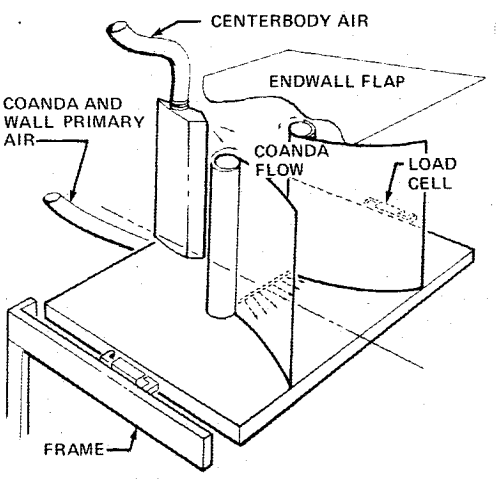

Fig. 5 Sketch of the test ejector.

Chordwise total and static pressure surveys were obtained at several streamwise and span stations by means of a traversing rake system on which was mounted a pitot-static probe. The resulting total and static pressure profiles were digitized, corresponding velocity values were calculated and plotted. The error in positioning the pitot-static probe has been estimated at $\pm 10\%$ of the hypermixing element length c.

B. Initial Conditions

The initial conditions for the velocities at the nozzle exit plane were primarily determined from experimental measurements. The mainstream jet velocity u was calculated from the measured mass flow for the hypermixing nozzle with the jet velocity component in the y direction v calculated using the calculated u velocity and the tangent of the hypermixing angle. The velocity components in the z direction w were set to zero initially.

Experimental secondary flow velocities were not available at the nozzle exit plane; however, they were available at the ejector throat. Since the inlet region from the nozzle exit to the throat is an accelerating flow region, an arbitrary contracting inlet shape was used as the boundary from the nozzle exit to the throat. Continuity was then used to calculate the correct secondary velocity given in the inlet boundary and the known experimental secondary velocity at the throat.

Specifying the initial v velocity components of the secondary flow was found to be necessary to obtain reasonable agreement with experimental velocity profiles at downstream locations approaching the diffuser exit. No cross-stream velocity components were measured in the experiment so the initial v velocity components in the secondary flow were determined by using the secondary u velocity and the tangent of the secondary flow direction angle. This angle was set equal to the hypermixing jet angle near the jet and linearly decreased to zero at a point midway between the jet and the adjacent ejector boundary.

Turbulence initial conditions for the jet were not known for the test configuration, so a value of initial turbulence kinetic energy based on freejet measurements was used. The initial level of turbulence kinetic energy in the jet was specified to be 12% of the jet mean flow kinetic energy. Decreasing the initial turbulence kinetic energy to 6% of the jet mean flow kinetic energy changed the computed mainstream velocities by less than 1%. The turbulence kinetic energy level in the initial secondary stream was set equal to 0.2% of the mean secondary flow kinetic energy. Changes in the initial levels of secondary flow turbulence also resulted in negligible changes in the computed results. The insensitivity to the initial turbulence levels leads to the conclusion that the magnitudes of the turbulence kinetic energy (and resulting flowfield development) are dominated by the streamwise vortex formed rather than the initial turbulence. The initial value of the dissipation ϵ was specified such that the resulting turbulent viscosity became equal to $0.0025\rho u_J t$ in the jet and $0.000025\rho u_J t$ in the secondary flow.

C. Computational Details

A grid of 25 points in the y direction and 22 points in the z direction was used for the computations. The grid points were unequally spaced with the highest density of points being in the vicinity of the hypermixing jet. Making the grid finer, 39×28, resulted in changes in local mainstream velocities of about 5%. The step sizes in the streamwise direction x were variable; they gradually increased with x and resulted in a total of about 60 steps from the inlet to the exit of the ejector. The solution for the 25×22 grid required an average of eight iterations per step to obtain convergence and a little less than 1 s per iteration on an IBM 370/168 computer.

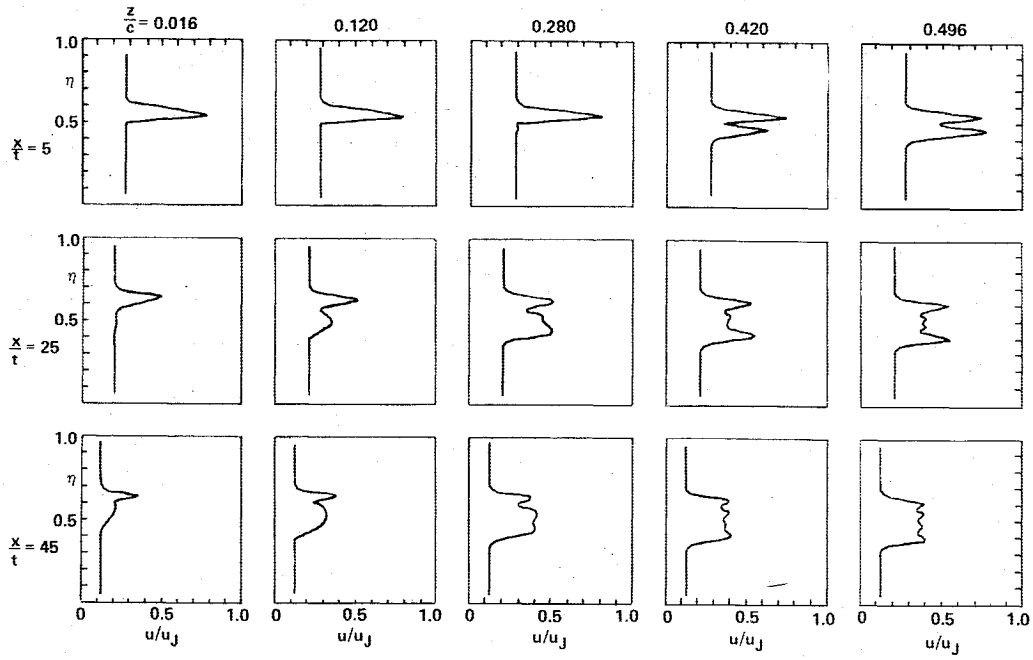

Fig. 6 Predicted mainstream velocity profiles.

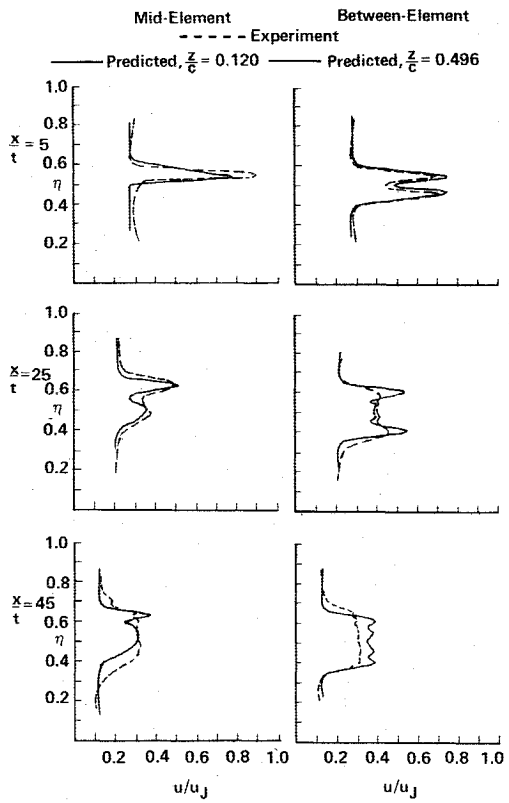

Fig. 7 Comparison of measured and predicted mainstream velocities.

D. Mainstream Velocity Profiles

Selected computed mainstream velocity profiles from the midelement ($z/c=0$) to the between-element plane ($z/c=0.5$) of an element with a positive v velocity component are presented in Fig. 6 at three x/t positions. The velocity profiles from $z/c=1.0$ to 0.5 (negative v velocity) , which are not shown, are the same as those presented from $z/c=0$ to 0.5 except that they are inverted with respect to $\eta=0.5$. At a low value of x, such as $x/t=5$, the jet profile is seen to develop from a single peak (located above $\eta=0.5$) at the midelement position to a double peak at the between-element position. At larger values of x, however, the two peaks of velocity are visible at almost all values of z. This is to be expected, because for these downstream locations the cross-stream velocities had enough opportunity to convect the second peak from the between-element location to the midelement location. That the flow created by the hypermixing jet would eventually become a two-dimensional flow is also indicated by the profiles for $x/t=45$. The magnitude of the secondary flow velocity is seen to decrease as x increases; this is the result of the area increase in the diffuser.

The computed velocity profiles are compared to measured profiles in Fig. 7. The computed profiles at $z/c=0.12$ are shown in the midelement comparison rather than one closer to $z/c=0$. The reason is that the measured profiles for the midelement location appeared to have a shape so much like the computed profiles at $z/c=0.12$ that the probe alignment was believed to be in error by the corresponding distance. After all, a small misalignment of the probe could cause a large change in the measured velocities, and detailed measurements at many z locations would be required to resolve this matter conclusively. Within the uncertainty of the probe alignment, the comparison of the predicted velocity profiles with the measured ones is considered to be satisfactory. All of the qualitative features such as the double peak between the elements, the appearance of the second peak at the midelement location and the merging of the two peaks at large values of x are correctly predicted; and the quantitative agreement between measurement and prediction is also fairly good.

E. Cross-Stream Velocity Field

The computed velocity vectors in the cross-stream plane are presented in Fig. 8 for three x/t locations. The computed results definitely show the development of streamwise vortex from the hypermixing nozzle. When the hypermixing nozzle concept was conceived, it was proposed that a vortex was developed but its existence was never really verified by any means. The present computations appear to be the first theoretical calculation of the streamwise vortex of the hypermixing jet. Figure 8 shows that the overall shape and pattern of the vortex is preserved at all x locations; but the magnitudes of the velocities decay with x.

F. Pressure Rise Through the Ejector

The predicted pressure rise through the ejector is compared to experimental data in Fig. 9. The pressure rise is un-

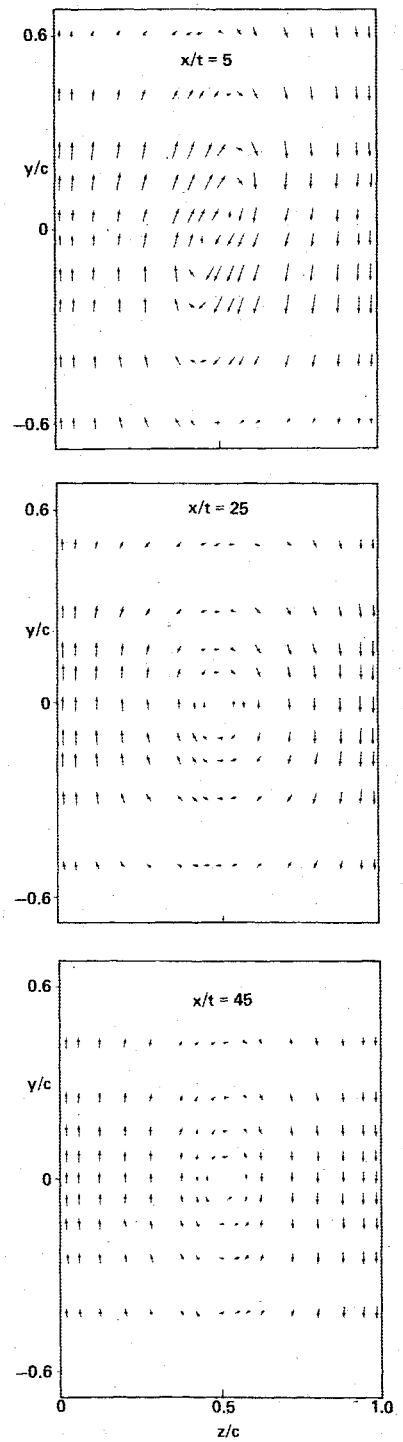

Fig. 8 Predicted cross-stream velocity field.

derpredicted by 7%. Here it must be remembered that the computations focused attention on the hypermixing jet and did not include the wall jets on the diffuser walls; also the friction at the diffuser walls was put equal to zero. The measured pressure rise is of course influenced by the presence of the wall jets and the wall friction. Some of the discrepancy in Fig. 9 can be attributed to these factors. With this perspective, the agreement between experiment and prediction can be judged to be satisfactory.

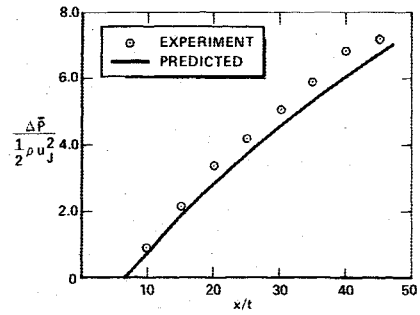

Fig. 9 Pressure rise in the ejector.

IV. Final Remarks

A three-dimensional parabolic finite-difference method incorporating a two-equation turbulence model has been used to predict the flowfield generated by a hypermixing jet in an ejector. The streamwise vortex formed by the jet has been predicted along with other important details of the flowfield. The comparison of the predictions with experimental data shows satisfactory agreement. It should be noted that the empirical constants in the turbulence model used have been previously established from other situations, and have *not* been adjusted for the particular problem considered here. The flowfield predictions have been found to be insensitive to the intitial levels of turbulence. This is a consequence of the substantial generation of turbulence kinetic energy caused by the streamwise vortex in the flowfield. The present study establishes confidence in the ability of the method described to predict the complex flow of a hypermixing jet in an ejector.

Acknowledgment

The authors would like to acknowledge the contribution of M. Seiler and P. Tu, who directed the experiments and thank P. M. Bevilaqua for his advice during this work.

References

[1] Bevilaqua, P. M., "Evaluation of Hypermixing for Thrust Augmenting Ejectors," *Journal of Aircraft*, Vol. 11, June 1974, pp. 348-354.

[2] Bevilaqua, P. M., "Analytic Description of Hypermixing and Test of an Improved Nozzle," *Journal of Aircraft*, Vol. 13, Jan. 1976, pp. 43-48.

[3] Quinn, B. P., "Compact Ejector Thrust Augmentation," *Journal of Aircraft*, Vol. 10, Aug. 1973, pp. 481-486.

[4] von Kármán, T., "Theoretical Remarks on Thrust Augmentation," *Contributions to Applied Mechanics, Ressner Anniversary Volume*, J. W. Edwards, Ann Arbor, Mich., 1949, pp. 461-468.

[5] Salter, G. R., "Method for Analysis of V/STOL Aircraft Ejectors," *Journal of Aircraft*, Vol. 12, Dec. 1975, pp. 974-978.

[6] Bevilaqua, P. M. and McCullough, J. K., "Entrainment Method for V/STOL Ejector Analysis," AIAA Paper 76-419, San Diego, Calif., July 1976.

[7] Gilbert, G. B. and Hill, P. G., "Analysis and Testing of Two-Dimensional Slot Nozzle Ejectors with Variable Area Mixing Sections," NASA CR-2251, 1973.

[8] Patankar, S. V. and Spalding, D. B., "A Calculation Procedure for Heat Mass and Momentum Transfer in Three-Dimensional Parabolic Flows," *International Journal of Heat and Mass Transfer*, Vol. 15, 1972, pp. 1787-1806.

[9] Launder, B. E. and Spalding, D. B., "The Numerical Computation of Turbulent Flows," *Computer Methods in Applied Mechanics and Engineering*, Vol. 3, March 1974, pp. 269-289.

[10] Spalding, D. B., "A Novel Finite-Difference Formulation for Differential Expressions Involving Both First and Second Derivatives," *International Journal of Numerical Methods in Engineering*, Vol. 4, 1972, p. 551.